

Serial Assessment of Renal Anatomy and Function in Mice with Unilateral Ureteral Obstruction Using Multi-modal Imaging

C. Chad Quarles¹, Feng Weng¹, Mohammed Tantawy¹, Rosie Jiang², Keiko Takahashi², Chuan-Ming Hao², Todd Peterson¹, Raymond Harris², and Takamune Takahashi²

¹Institute of Imaging Science, Vanderbilt University, Nashville, TN, United States, ²O'Brien Mouse Kidney Physiology and Disease Center, Vanderbilt University, Nashville, TN, United States

Introduction: The application of non-invasive imaging techniques in mouse models of renal disease could be useful for the serial evaluation of the functional, structural, and metabolic changes which occur during disease progression. The goal of this study was to systematically optimize high-field, high-resolution T₁, T₂ and Magnetization Transfer Contrast (MTC) MRI and ^{99m}Tc-mercaptoacetyltryglycine (^{99m}Tc-MAG3) scintigraphy for mouse renal imaging and apply them to investigate the anatomical and functional changes that occur following unilateral ureteral obstruction (UO).

Methods: Multi-modality images of mice were acquired using a 7T MRI scanner and a NanoSPECT/CT system. The imaging parameters for each modality were optimized in cohorts of control mice. For MRI, the pulse sequence selection, parameters and use of respiratory gating, navigator echos and fat saturation were all optimized to enhance image contrast between the cortex and medulla. Once optimized, imaging data was acquired in sham operated (n = 8) and UO mice (n = 8) at 0 (3 hours), 1, 3 and 6 days after surgery. Histology was acquired in separate cohorts of UO mice. For ^{99m}Tc-MAG3, Time-Activity Curves (TACs) were produced for each kidney and relative renal blood flow (rRBF) and functional parameters were assessed using the slope of ^{99m}Tc-MAG3 influx, peak activity, and the time-to-peak (TTP).

Results: Figure 1 shows example T₁- and T₂-weighted MR images of a UO mouse at 0, 1, 3 and 6 days post-surgery. The renal pelvic space was gradually expanded in obstructed kidneys as early as 1 day post ureteral ligation and the components of renal medulla, especially inner medulla and papilla, was remarkably decreased as the disease progressed. Reduction of renal cortex was also observed at day 3 and day 6. Histological investigation displayed typical patterns of UO renal disease including tubular dilatation, flattening, and atrophy, and expansion of interstitial area with extracellular matrix accumulation and infiltration of inflammatory cells. Tubulointerstitial region progressed markedly over 6 days after ureteral obstruction. Obvious structural changes were not observed in contra-lateral kidneys and sham operation mouse kidneys. The MTC data analysis is currently underway.

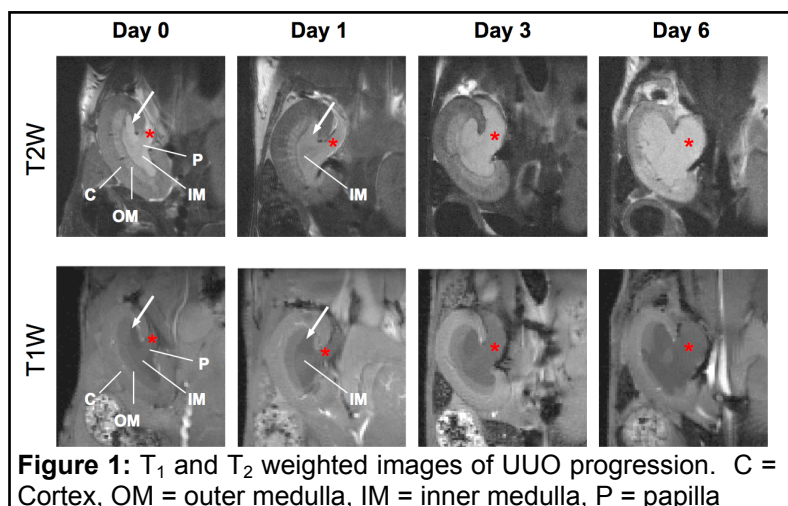


Figure 1: T₁ and T₂ weighted images of UO progression. C = Cortex, OM = outer medulla, IM = inner medulla, P = papilla

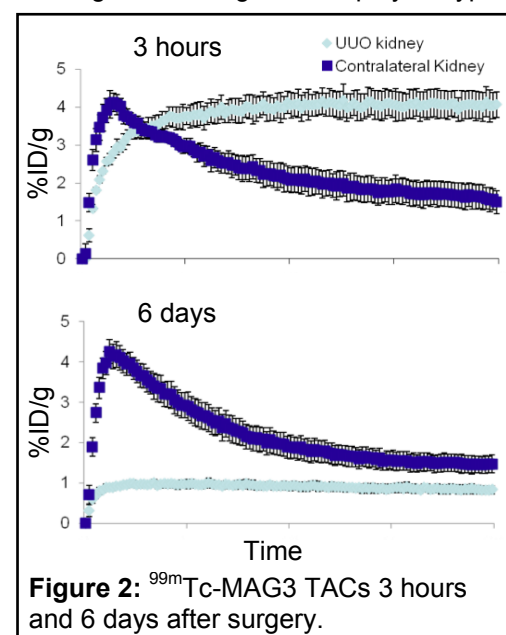


Figure 2: ^{99m}Tc-MAG3 TACs 3 hours and 6 days after surgery.

Figure 2 shows example ^{99m}Tc-MAG3 TACs 3 hours and 6 days after surgery. Compared to sham mice, rRBF was remarkably (>60%) reduced in UO kidneys as early as day 1 post-surgery and the TACs plateaued, indicating that ^{99m}Tc-MAG3 is not excreted in these kidneys. The plateau activity in UO kidneys was relatively low (~40% of sham kidney's peak activity) and the time to plateau exceeded 200 sec, indicating reduced functional vessels and slow perfusion. Conversely, rRBF was progressively increased in contra-lateral kidneys, exhibiting a ~130% increase at day 6, although peak activity and TTPs were minimally changed. These data demonstrate that renal perfusion is remarkably and rapidly reduced in UO kidneys, whereas it is gradually increased in contra-lateral kidneys.

Conclusion: In pre-clinical models of renal disease, these imaging techniques could be effective tools for screening pharmacological agents and for elucidating pathological mechanisms of obstructive kidney disease.

Acknowledgements: NIDDK 1P30 DK079341